Light and oxygen are not required for harpin-induced cell death

Marie Garmier, Pierrick Priault, Guillaume Vidal, Simon Driscoll, Reda Djebbar, Martine Boccara, Chantal Mathieu, Christine H. Foyer, Rosine de Paepe

HAL Id: hal-02656768

https://hal.inrae.fr/hal-02656768v1

Submitted on 30 May 2020

Light and Oxygen Are Not Required for Harpin-induced Cell Death*

Marie Garmier[‡1], **Pierrick Priault**[§1,2], **Guillaume Vidal**[‡1], **Simon Driscoll**[¶], **Reda Djebbar**[∥], **Martine Boccara**[**],
Chantal Mathieu[‡], **Christine H. Foyer**[¶], and **Rosine De Paepe**[‡3]

From the [‡]*Institut de Biotechnologie des Plantes, Université Paris-Sud 11, UMR-CNRS 8618, Bâtiment 630,
91405 Orsay cedex, France,* [§]*Ecologie, Systématique et Evolution, Université Paris-Sud 11, UMR-CNRS 8079, Bâtiment 362,
91405 Orsay cedex, France,* [¶]*School of Agriculture, Food, and Rural Development, Agriculture Building, Newcastle University,
Newcastle upon Tyne, NE1 7RU, United Kingdom,* [∥]*Laboratoire de Physiologie Végétale, Faculté des Sciences Biologiques,
Université des Sciences et de la Technologie Houari Boumedienne, BP 39, El Alia, Bab Ezzouar, 16111 Alger, Algeria,*
[**]*Atelier de Bioinformatique, Université Pierre et Marie Curie Paris 6, 12 Rue Cuvier, Paris 75005, France*

Nicotiana sylvestris **leaves challenged by the bacterial elicitor harpin** N_{Ea} **were used as a model system in which to determine the respective roles of light, oxygen, photosynthesis, and respiration in the programmed cell death response in plants. The appearance of cell death markers, such as membrane damage, nuclear fragmentation, and induction of the stress-responsive element** *Tnt1*, **was observed in all conditions. However, the cell death process was delayed in the dark compared with the light, despite a similar accumulation of superoxide and hydrogen peroxide in the chloroplasts. In contrast, harpin-induced cell death was accelerated under very low oxygen (<0.1% O_2) compared with air. Oxygen deprivation impaired accumulation of chloroplastic reactive oxygen species (ROS) and the induction of cytosolic antioxidant genes in both the light and the dark. It also attenuates the collapse of photosynthetic capacity and the respiratory burst driven by mitochondrial alternative oxidase activity observed in air. Since alternative oxidase is known to limit overreduction of the respiratory chain, these results strongly suggest that mitochondrial ROS accumulate in leaves elicited under low oxygen. We conclude that the harpin-induced cell death does not require ROS accumulation in the apoplast or in the chloroplasts but that mitochondrial ROS could be important in the orchestration of the cell suicide program.**

Light and oxygen are generally considered to be important in the responses of plants to environmental stress, principally because they are involved in the generation of reactive oxygen species (ROS)[4]

and associated molecular and biochemical changes. ROS are central to redox sensing during biotic and abiotic stress responses, and they act as second messengers in the activation of signal transduction pathways. ROS activate mitogen-activated protein kinase cascades that phosphorylate a variety of proteins involved in plant growth and development as well as death responses (1). High ROS levels can trigger the appearance of programmed cell death (PCD) and the induction of caspase activation in animals (2) and the activation of the ubiquitin/26 S proteasome system in plants (3). The cellular compartmentation of ROS production in PCD responses has been extensively investigated. For example, it has been established that ROS are generated in the apoplast during the oxidative burst that often accompanies plant PCD responses (4). It is widely accepted that this oxidative burst is caused by activation of DPI-sensitive NADPH oxidase-like enzymes (5) and/or the activation of various extracellular oxidases and peroxidases (6) linked to the spontaneous or enzyme-catalyzed dismutation of superoxide to H_2O_2. However, clear cause and effect relationships between apoplastic ROS production and the execution of cell death have never been established, and ROS have been suggested to be involved in the spread of cell death rather than in the death process *per se* (7).

Other possible sites of ROS production are the chloroplasts and mitochondria. The photosynthetic electron transfer chain (ETC) in the chloroplasts is the major site of ROS generation in photosynthetic cells. Thus, light and chloroplast-based reactions as well as the associated process of photorespiration are considered to have a predominant role in cellular redox regulation (8, 9). Exposure to abiotic stresses, such as drought, frequently causes inhibition of photosynthesis and accelerated ROS production (10). Pathogen attack causes suppression of photosynthetic gene expression (11) and a concomitant inhibition of photosynthesis (12, 13), suggesting that light and ROS trigger common signaling pathways in plants exposed to abiotic and biotic stresses (14, 15). Although ROS production by the mitochondrial ETC represents less than 1% of chloroplastic ROS generation in photosynthetic tissues (16), mitochondria have been proposed to be as important in the establishment of

[4] The abbreviations used are: ROS, reactive oxygen species; PCD, programmed cell death; ETC, electron transfer chain; AOX, alternative oxidase;

VLO, very low oxygen; NBT, nitro blue tetrazolium; DAB, 3,3'-diaminobenzidine; pi, postinfiltration; PSII, photosystem II; SOD, superoxide dismutase.

cell death in plants as they are in animals (17). Cytochrome *c* release, a hallmark of animal cell death (18), has been observed during plant cell death (19). Mitochondrial superoxide production is restricted by the activity of alternative oxidase (AOX), a cyanide-resistant terminal oxidase (20). The abundance of *AOX* transcripts and proteins is increased when plants are subject to a range of stresses (21, 22), and the induction of AOX activity has been observed *in planta* during elicitor-induced cell death (23).

The aim of the present work was to explore the role of ROS in elicitor-induced cell death by using very low oxygen conditions to diminish the activity of enzymes involved in ROS accumulation in different cellular compartments and dark conditions to prevent ROS production by the chloroplastic ETC. We used the bacterial protein harpin N_{Ea} infiltrated into *Nicotiana sylvestris* leaves as a model system for elicitor-induced PCD. The harpin N_{Ea} protein is produced by *Erwinia amylovora*, the causative agent of fire blight disease in Rosaceae, which induces cell death in leaves of nonhost plants, such as tobacco and *Arabidopsis* (24). Harpin proteins are secreted by Gram-negative bacteria via a type III secretion apparatus (25). *E. amylovora* mutants devoid of harpin N_{Ea} secretion show both lower virulence in host species and reduced cell death in nonhost plants (26). Harpins induce apoplastic ROS accumulation (27), activation of kinase signaling (28) and systemic acquired resistance (SAR) in nonhost plants (29). The elicitation of defense responses by harpins in cultured cells is an active process that is inhibited by cycloheximide and calcium channel blockers (30). Interestingly, harpins differentially alter mitochondrial function in plant cell suspension cultures (31, 32) and leaves (23), suggesting an important role for mitochondria-chloroplast interactions in the death response.

Here we show that harpin N_{Ea}-induced cell death is executed in *N. sylvestris* leaves under conditions of atmospheric oxygen (air; 21% O_2) or under very low oxygen (VLO; <0.1% O_2). Similarly, the elicitation of PCD markers is observed in the light and in the dark. However, the kinetics of the cell death process are accelerated by light and, more unexpectedly, by VLO. The respiratory and photosynthetic signatures associated with the cell death response were followed together with nuclear morphology, intracellular localization of ROS accumulation, and the expression of cell death markers and antioxidant genes.

EXPERIMENTAL PROCEDURES

Plant Growth Conditions—Seeds of *N. sylvestris*, the diploid maternal ancestor of *Nicotiana tabacum*, were provided by the Institut des Tabacs (Bergerac, France). Plants were grown in soil in a greenhouse under natural lighting, supplemented by artificial lighting (Philips SON-7 AGRO 400 W lamps) at a day/night temperature of 23.5 °C/17.5 °C and a day/night 60%/50% relative humidity. Plants were irrigated with nutrient solution (Hydrokani C₂Hydro Agri Spécialités, France).

Harpin$_{Ea}$ Isolation and Leaf Infiltration—Harpin$_{Ea}$ was isolated from cell-free culture supernatants from *Escherichia coli* DH5α, which had been transformed with plasmid pCPP430 carrying the cloned HrpN$_{Ea}$ gene (a gift from Dr. M. A. Barny, Institut National de la Recherche Agronomique, France), as described in Ref. 33. Prior to infiltration with buffer or harpin,

leaves were acclimated for 30 min under 0.1 or 21% oxygen (VLO and air, respectively), in both the light and the dark, in a multichamber system (IACR, Rothamsted) or into the chamber of a Licor 6400-40 infrared gas analysis system, as described under "Steady-state CO_2 Exchange and Fluorescence Measurements." A 0.1-ml volume of harpin at a concentration of 40 μg ml^{-1} in TE buffer (10 mM Tris, pH 7.5, 0.1 mM EDTA) was infiltrated with a hypodermic syringe into the abaxial face of the second fully expanded leaf of 6–8-week-old plants. The infiltrated zones were thereafter immediately replaced in the gas chambers. Sampling for electrolyte leakage, RNA extraction, and cytological studies was performed at the indicated times. Using Licor, care was taken to harvest samples from the inside of the gas chamber.

Electrolyte Leakage Measurements—At different times after harpin or buffer infiltration, eight discs were punched out from treated tissues with a core borer (0.5-cm diameter) and placed in 10 ml of sterile distilled water. Electrolyte leakage using a CD60 "resistivimeter" (Tacussel Electronique, France) was measured as described in Ref. 34. Results were expressed as percentage of leakage obtained after 10 min of incubation of leaf discs at 95 °C.

Nuclear Morphology—Leaf discs (1.3 cm²) were harvested after the different treatments and vacuum-infiltrated (30 min at room temperature) with 50 mM potassium phosphate (pH 8) containing 4% paraformaldehyde. Samples were washed twice with 50 mM potassium phosphate buffer (pH 8). Cells were then dissociated by incubation at 60 °C in 0.1 M EDTA (pH 9) for 90 min and then maintained at 4 °C until analysis. Nuclei stained with the fluorochrome Hoechst 33342 (Sigma) were observed using epifluorescence microscopy (Zeiss). Picture acquisitions were made using a numeric camera RT SPOT (Diagnostic Instrument, Inc.) and associated software.

Steady-state CO_2 Exchange and Fluorescence Measurements—Gas exchange measurements were performed using an infrared gas analyzer (model wa-225-mk3; ADC, Hoddesdon, Hertfordshire, UK) as described in Ref. 35. Once steady-state leaf dark respiration rates had been attained in the chambers, respiratory CO_2 release was monitored for 20 min prior to illumination. Leaves were illuminated at 350 μmol quanta m^{-2} s^{-1} until steady-state rates of CO_2 uptake were reached. The gas composition was controlled by a gas mixer supplying CO_2 and O_2 at the stated concentrations with the balance made up with N_2. Leaves were then infiltrated with either buffer or harpin, and gas exchange measurements began again immediately. Leaf temperatures were maintained by water jackets at 23 °C. Alternatively, infiltrated areas were placed in the leaf chamber of the Licor 6400-40 infrared gas analysis system (Li-Cor Corp., Lincoln, NE). Gases were maintained at stable concentrations with 0.038% CO_2 (via two soda lime columns associated with the Licor system) and either 21% O_2 (air) or 0.1% O_2 (VLO) by using a highly purified N_2 gas bottle (industrial quality I grade; Air Liquide, France). In the "dark" experiments, leaves were initially dark-adapted for at least 30 min under both air and VLO conditions. Chlorophyll *a* fluorescence parameters were measured in an on-line system with minimal and maximal fluorescence (F_o and F_m) values recorded every 3 min. In the "light" experiments, steady state photosynthesis rates were measured

under 350 μmol quanta m^{-2} s^{-1} actinic light for at least 1 h under both air and VLO concentrations prior to chlorophyll *a* fluorescence analysis, and then measurements were made continuously throughout the course of the experiment. Fluorescence parameters of light-adapted leaves were measured every 3 min and the following parameters were calculated according to Refs. 36 and 37: the maximum yield of PSII photochemistry ($F_v/F_m = (F_m - F_o)/F_m$), the quantum yield of electron flow through photosystem II (ΦPSII $= (F'_m - F_t)/F'_m$) and the photochemical quenching of chlorophyll fluorescence ($qP = (F'_m - F_t)/(F'_m - F'_o)$). The parameter ($1 - qP$) is a measure of the fraction of closed photosystem II reaction centers.

Cytological Detection of ROS—The accumulation of superoxide (O_2^-) and hydrogen peroxide (H_2O_2) was monitored *in situ* using nitro blue tetrazolium (NBT) and 3,3'-diaminobenzidine (DAB), respectively, as described in Ref. 38. The leaf discs were vacuum-infiltrated (three cycles of 5 min) with a solution of NBT (81 mM) in 10 mM potassium phosphate buffer (pH 7.8) or with 36 mM aqueous DAB (pH 3.8). After incubation in the dark at room temperature (1 h and 14 h for each stain, respectively), the leaf samples were incubated in 90% ethanol at 70 °C until all of the chlorophyll had been completely removed. The samples were then cleared by incubation overnight in an 8:2:1 chloral hydrate solution (chloral hydrate (w/v), H$_2$O (v/v), glycerol (v/v)) at room temperature. Microscopic images were taken using a Zeiss microscope. Photographic images were produced using a numeric camera RT SPOT (Diagnostic Instrument) and the relevant accompanying software.

RNA Isolation and Gel Blot Analysis—Leaf tissue pieces were frozen in liquid nitrogen, and total RNAs were extracted by the Trizol-chloroform procedure (Invitrogen). Aliquots (10 μg) of total RNA were subjected to Northern blot analyses as described in Ref. 38.

Statistical Analysis—Data were compared using analysis of variance statistical analysis at the $P_{0.05}$ level of significance (STATISTICA software; STATSOFT Inc., Tulsa, OK), unless specified. Data are expressed as the means ± S.E.

RESULTS

The Time Course of Harpin-induced Cell Death Is Not Impaired by Oxygen Deprivation or by Darkness—The visible symptoms associated with the harpin-induced cell death response, such as changes in the translucency of the infiltrated area were first observed at ~5–6 h postinfiltration of leaves, leading to complete necrosis at 48 h pi regardless of the conditions of oxygen availability and illumination (Fig. 1). Infiltration of the leaves with buffer alone did not produce necrotic symptoms. The kinetics of the cell death process was quantified by two methods: alterations in fresh weight and electrolyte leakage (Fig. 2). The latter technique has been used previously as a cell death marker *in planta* (34). Any excess liquid occupying the intercellular spaces had evaporated within about 1 h of infiltration in illuminated harpin-treated leaves in air (Fig. 2*A*), similar to the situation in buffer-treated leaves (not shown). The fresh weight values of the elicited leaf area had decreased by about 20% at the 4 h time point compared with preinfiltration values, by 40% at 8 h pi, and by 80% at 24 h pi. In dark-elicited leaves, tissue dehydration was delayed when compared with illumi-
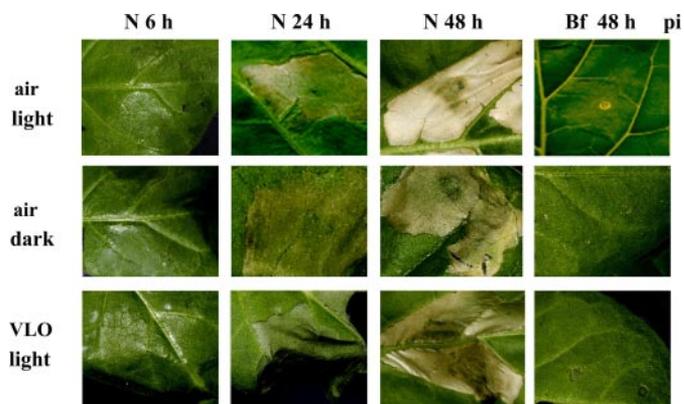

FIGURE 1. **Cell death symptoms in leaf areas infiltrated with harpin under different environmental conditions.** Leaves were infiltrated in the dark and the light, and under atmospheric and VLO conditions, as described under "Experimental Procedures." Infiltrated areas are shown at 6, 24, and 48 h post-harpin infiltration (*N*), and at 48 h postbuffer infiltration (*Bf*) (h pi).
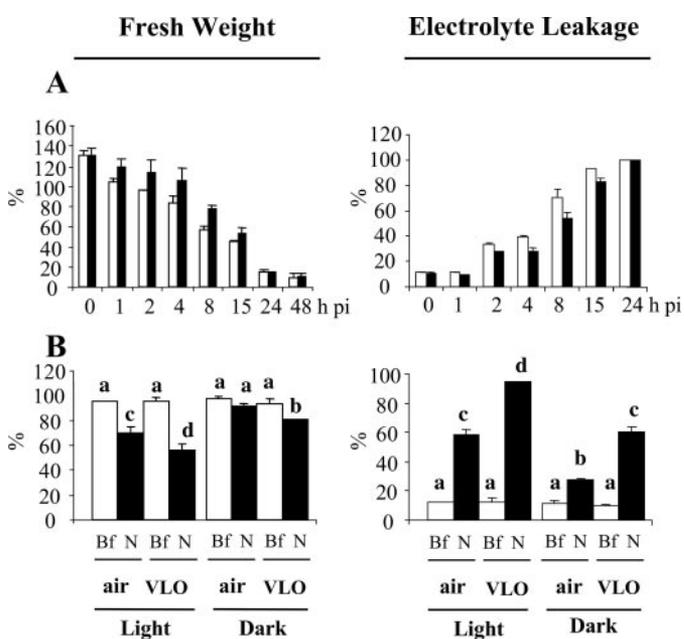

FIGURE 2. **Fresh weight and electrolyte leakage in harpin-elicited tissues under various conditions.** *A*, a comparison of harpin elicitation in the light (350 μmol m^{-2} s^{-1}) and in the dark during the cell death process under air. *Open columns*, light; *closed columns*, dark. *B*, a comparison of harpin (*N*) and buffer (*Bf*) infiltration under air and VLO (<0.1% O$_2$) at the 5 h pi, under light or dark conditions. *Open columns*, buffer; *closed columns*, harpin N. Electrolyte loss is presented as a percentage of that occurring under conditions of total membrane destruction (after incubation of leaf discs for 10 min at 95 °C) and dehydration (calculated as a percentage of the fresh weight of a nontreated leaf disc) in harpin- and/or buffer-treated tissues. Values are the means of at least three independent experiments. *B*, statistically different values at the $p < 0.05$ level (analysis of variance, Fisher's least significant difference test) are indicated by different *letters*.

nated leaves. The intercellular liquid evaporation took about 4 h, and the fresh weight remained at higher values than those of illuminated leaves up to 8 h pi ($p < 0.01$). At the 24 h time point, however, the fresh weight was only about 15% of the initial values in both dark- and light-elicited leaves. The delay in water loss observed in dark-elicited tissues was probably due to the lower stomatal aperture under these conditions (39). However, a similar delay in electrolyte leakage was observed in dark-elicited leaves (Fig. 2*B*, $p < 0.05$), thereby indicating that the progression of the cell death execution process *per se* was less
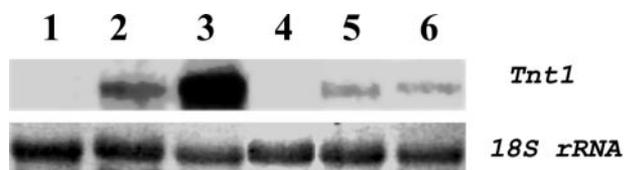
FIGURE 3. **Accumulation of *Tnt1* transcripts in leaf areas infiltrated with harpin in different environmental conditions.** Shown are Northern blot analyses of *Tnt1* transcript accumulation, 4 h post-harpin infiltration. *Lane 1*, untreated leaf in the light and under air; *lane 2*, harpin 4 h pi, in the light and under air; *lane 3*, harpin 4 h pi, in the light and under VLO; *lane 4*, untreated leaf in the dark and air; *lane 5*, harpin 4 h pi, in the dark and under air; *lane 6*, harpin 4 h pi, in the dark and under VLO. The 18 S rRNA was detected as a standard for relative loading. Results shown are representative of three independent experiments.

rapid in the dark than in the light. Maximum rates of ion leakage were observed 24 h pi in both conditions, indicating that most of the cells have lost membrane integrity at this time point.

Both water loss and electrolyte leakage were accelerated under VLO when compared with air, in both the light and the dark (Fig. 2*B*). At 24 h pi, the loss of membrane integrity following harpin treatment was comparable in all conditions (data not shown). No visible symptoms, significant electrolyte leakage, or water loss were observed in untreated leaves (data not shown) or buffer-infiltrated leaves (Fig. 2*B*) in either conditions. These results show that oxygen deprivation *per se* did not induce cell death in tobacco leaves over the time period of the present study. It is well known that, in contrast to animal cells, plant cells are able to survive to severe hypoxia for several h (40).

The induction of the tobacco *Tnt1* transposon expression was chosen as a molecular marker for the progression of the elicitation under the different conditions. *Tnt1* transcripts have previously been shown to accumulate under various stress conditions, particularly in tobacco suspension cells following exposure to *Erwinia chrysanthemi* supernatants (41). *Tnt1* transcripts were more abundant under VLO than in air 4 h post-harpin inoculation in the light, and their accumulation was lower in the dark than in the light under both air and VLO conditions (Fig. 3).

Nuclear fragmentation is a hallmark of PCD in animals (42). We therefore compared the extent of nuclear fragmentation in dissociated cells of untreated and harpin-infiltrated leaves stained using the Hoechst fluorochrome system. In untreated leaves maintained in the different environmental conditions, including 24 h under VLO, the vast majority of nuclei (about 95%) were round in shape in all of the cell types examined (parenchyma as well as epidermal and guard cells) (Figs. 4, *A* and *D*, and 5). No marked changes in nuclear morphology were observed in cells treated with buffer or with harpin until 12 h pi in air (data not shown). However, at 24 h post-harpin inoculation in air in the light and in the dark, about 40% of the nuclei were found to be deformed with signs of fragmentation (Figs. 4, *B* and *H*, and 5). In contrast, the proportion of deformed and/or fragmented nuclei was around 80% under VLO at 24 h pi, in the light (Figs. 4*E* and 5) and in the dark (not shown). Nuclear fragmentation was especially pronounced in stomatal guard cells (Figs. 4*E* and 5). At 48 h pi, most cells were devoid of visible nuclei in all conditions (Fig. 4, *C*, *F*, and *I*), and 85% (air) to 95% (VLO) of the remaining nuclei were fragmented (Fig. 5). Inter-
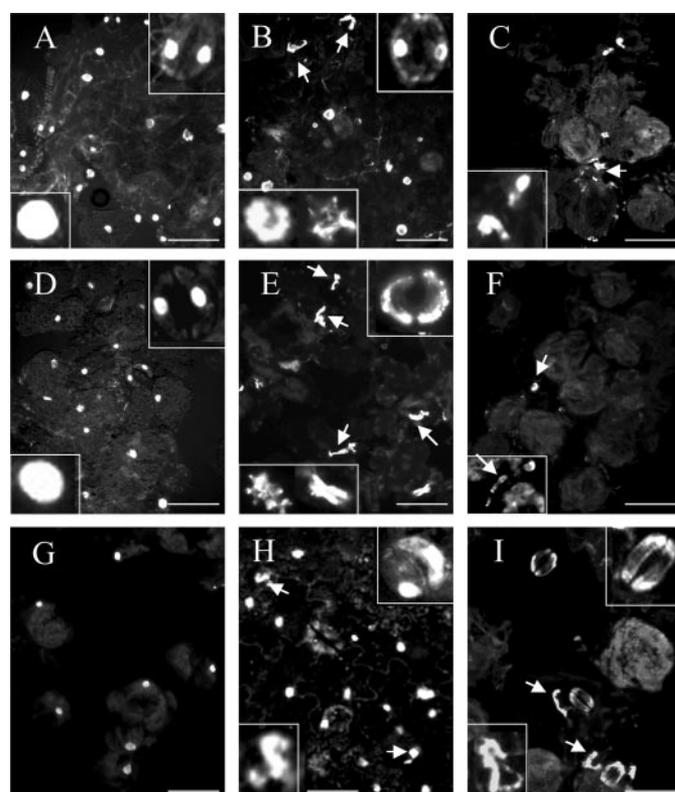
FIGURE 4. **Nuclear fragmentation in leaves infiltrated with harpin under different environmental conditions.** Cells were dissociated as described under "Experimental Procedures," and nuclei were stained using Hoechst fluorochrome. *White arrows*, fragmented nuclei. *White bars*, 100 μM. *A*, untreated leaves maintained under atmospheric oxygen (air) conditions in the light. *Bottom left inset*, enlargement ($\times$5) of a typical nucleus; *top right inset*, enlargement ($\times$5) of a representative stomata with two round shaped nuclei. *B*, leaves infiltrated with harpin in the light under air, 24 h pi. *Bottom left inset*, enlargement ($\times$3) of two representative fragmented nuclei; *top right inset*, enlargement ($\times$5) of a representative stomata, in which the two guard cell nuclei have a normal configuration. *C*, leaves infiltrated with harpin in the light under air, 48 h pi. *Inset*, enlargement ($\times$5) of two representative fragmented nuclei. *D*, untreated leaves maintained for 24 h under VLO in the light. *Bottom left inset*, enlargement ($\times$5) of a typical nucleus with a normal round structure; *top right inset*, enlargement ($\times$5) of a representative stomata. *E*, leaves infiltrated with harpin in the light under VLO, 24 h pi. *Bottom left inset*, enlargement ($\times$5) of two representative fragmented nuclei; *top right inset*, enlargement ($\times$5) of a representative stomata, in which both nuclei are fragmented. *F*, leaves infiltrated with harpin in the light under VLO, 48 h pi. *Inset*, enlargement ($\times$5) of a fully fragmented nucleus. *G*, leaves infiltrated with cantharidin, in the light under air, 48 h pi. *H*, leaves infiltrated with harpin in the dark under air, 24 h pi; epidermal cells can be seen. *Bottom left inset*, enlargement ($\times$5) of a fragmented nucleus; *top right inset*, enlargement ($\times$5) of a representative stomata, in which the nucleus of one guard cell has a normal appearance, whereas the nucleus of the second cell is fragmented. *I*, leaves infiltrated with harpin in the dark under air, 48 h pi. *Bottom left inset*, enlargement ($\times$5) of a fragmented nucleus; *top right inset*, enlargement ($\times$5) of a representative stomata, in which nuclei are heavily degraded.

estingly, nuclear morphology was essentially unaffected in dead leaf areas 48 h postinfiltration with cantharidin (Fig. 4*G*), a phosphatase inhibitor (43) inducing a rapid necrotic process in *N. sylvestris* leaves under our experimental conditions (not shown).

Taken together, these observations demonstrate that light and oxygen modulate harpin-induced cell death in an inverse manner, the absence of light delaying the onset of the response, whereas oxygen deprivation accelerates the process. However, the general characteristics of the cell responses to harpin (electrolyte leakage, induction of *Tnt1* expression, and nuclear frag-
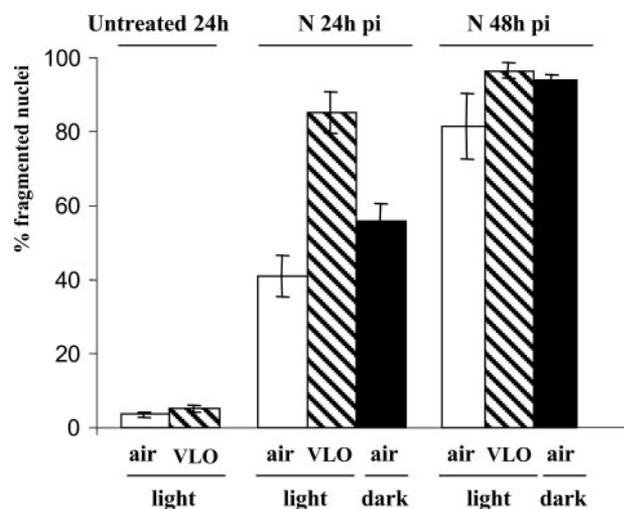
FIGURE 5. **Relative proportions of fragmented nuclei.** Cells of untreated or harpin- treated leaves were stained with Hoechst as in Fig. 4. Data are means and S.E. of 3–5 independent experiments. At least 100 nuclei (including guard cell nuclei) were examined at 24 h pi, and 50 nuclei were examined at 48h pi in each experiment. *Open columns*, air and light; *hatched columns*: VLO and light; *closed columns*, air and dark. The proportions (percentages) of fragmented nuclei at 24 h pi were significantly different between air and VLO.

mentation) were qualitatively the same under all conditions, suggesting that a similar type of cell death process was elicited.

Very Low Oxygen Tempers the Harpin-induced Impairment of Photosynthesis—In order to gain further insights into the relative contributions of events occurring in the chloroplasts and mitochondria in the execution of cell death, we compared CO_2 exchange rates and chlorophyll *a* fluorescence parameters in the different conditions (Fig. 6). Infiltration with either buffer or harpin in air caused an immediate collapse of CO_2 assimilation by illuminated leaves (Fig. 6*A*). This nonspecific effect was probably due to the limitations on gas diffusion caused by the presence of liquid in the intracellular spaces of infiltrated areas. As the liquid evaporated or was absorbed into the cytoplasm, the rates of net photosynthesis (An) increased to reach nearly initial values, a process that was completed within less than 2 h of infiltration. Subsequently, CO_2 assimilation progressively declined in the harpin-elicited leaves, such that the photosynthesis rates had virtually collapsed by 6 h pi. Stomatal conductance (g_s) immediately collapsed following buffer infiltration, recovered close to maximal values at around 2 h pi and then slightly decreased from 4 h pi onward (Fig. 6*B*). A bimodal pattern of increase and decrease in g_s was observed following harpin inoculation. Interestingly, g_s markedly increased from 3 to 6 h pi, at a time when net assimilation (An) was already severely affected. This indicates that decreased g_s was not the primary cause of the harpin-induced inhibition of photosynthesis. Rather, An inhibition was closely followed by a progressive decrease in PSII efficiency, as determined by ΦPSII (Fig. 6*C*). Evidence for the closure of PSII centers was also provided by the increase in $(1 - qP)$, which suggests a progressive reduction of the plastoquinone pool in harpin-elicited leaves (Fig. 6*D*).

The harpin-induced inhibition of An, PSII function, and g_s, as well as the rise in the $(1 - qP)$ parameter, were delayed under VLO compared with air (Fig. 6, *E–H*). These results indicate

that the photosynthetic process and the electron transport were partially protected from inhibition in the absence of oxygen.

Low Oxygen Impairs CO_2 Release in Dark-elicited Leaves—The CO_2 release by dark-elicited leaves increased from 2 h post-harpin inoculation, and maximum values, about 2.5 μmol m^{-2} s^{-1}, were observed at 4–8 h pi (Fig. 7*A*). This increase preceded any significant water loss, electrolyte leakage, or other symptoms (Figs. 1 and 2). Moreover, it was not observed in buffer-treated areas, indicating that it was not caused by liquid infiltration. From 10 h pi, rates of CO_2 release were about 2-fold higher in harpin-infiltrated than in buffer-infiltrated leaves. In addition, chlorophyll *a* fluorescence measurements indicated that harpin caused a progressive decrease in the dark-adapted F_v/F_m values (Fig. 7*B*), confirming that PSII reaction centers became progressively closed as a result of harpin treatment. Under VLO, the harpin-induced CO_2 burst was strikingly diminished in size and duration, although the values for CO_2 release remained about 2-fold higher in harpin-infiltrated than in buffer-infiltrated leaves up to 6 h pi (Fig. 7*C*). The decrease in the dark-adapted F_v/F_m ratios was attenuated under VLO and was observed in both buffer and harpin-treated zones (Fig. 7*D*). However, it was partially reversible by returning to air at the 7 h time point in buffer-, but not in harpin-infiltrated zones, suggesting that the harpin-mediated inhibition proceeds via an irreversible structural alteration of PSII reaction centers.

ROS Accumulation in Chloroplasts of Harpin-elicited Leaves Is Prevented by Low Oxygen but Not by Darkness—To investigate how harpin elicitation affects ROS accumulation in the different cellular compartments, we used NBT and DAB staining that monitor superoxide and hydrogen peroxide accumulation, respectively. The DAB reaction with hydrogen peroxide is catalyzed by peroxidases in all of the compartments of the plant cell, including the apoplast. However, it is generally assumed that cellular peroxidase activities are not limiting for the reaction, and thus the DAB system is generally considered to be a sensitive indicator of cellular hydrogen peroxide accumulation (44). The leaf veins became rapidly stained with NBT after harpin inoculation in both the light and the dark in air (Fig. 8). However, the extent of harpin-induced superoxide accumulation around the veins was not harpin-specific and was also observed in buffer-treated leaves (Fig. 9, *A* and *B*). Superoxide accumulation around vascular bundles has already been described under high light stress (45). From 2–3 h pi, numerous localized blue spots were observed in the mesophyll tissues, in much higher abundance in harpin- (Fig. 8) than in buffer-infiltrated zones (not shown). The intensity of NBT staining was greatest in the mesophyll cells at 4–5 h post-harpin infiltration, whereas the blue vein coloration had vanished at this time point (Fig. 8). From the 6–7 h pi onward, the NBT coloration became more diffuse and ultimately disappeared. The tissue distribution and progression of harpin-specific NBT staining was similar in dark- and in light-elicited leaves, although the time taken for the stain to reach maximum intensities was slightly delayed in the dark. In contrast, NBT staining was markedly attenuated in zones elicited under VLO, in both the dark and the light (Fig. 8).

In the experiments using DAB staining, the brown coloration started to develop at about 1 h post-harpin inoculation in illu-
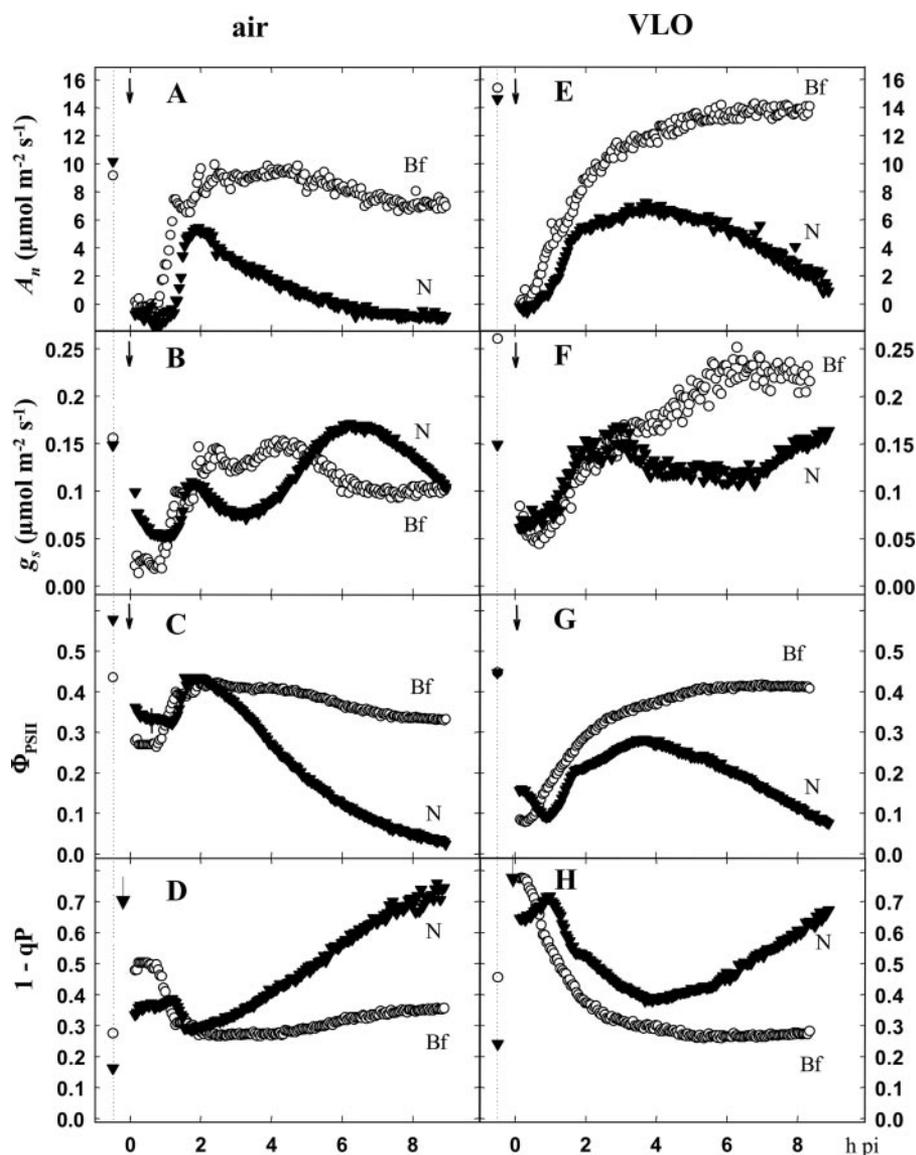
FIGURE 6. Photosynthetic and fluorescence parameters in leaves infiltrated in the light. After parameter stabilization (*first symbols* on the *vertical dashed line*) under 350 μmol quanta m^{-2} s^{-1} and air or VLO conditions, leaves were harpin- or buffer-infiltrated, and treated areas were immediately placed in the gas chambers, as described in under "Experimental Procedures." *Arrows*, time infiltration. Data from three independent experiments have been pooled. *Open circles*, buffer (*Bf*); *closed triangles*, harpin (*N*). *A–D*, air; *E–H*, VLO. *A* and *E*, CO$_2$ assimilation (A_n); *B* and *F*, stomatal conductance (g_s); *C* and *G*, ΦPSII (quantum yield of photosystem II); *D* and *H*, $1 - qP$ (fraction of closed PSII reaction centers).

increased markedly in both light-elicited and dark-elicited leaves. By 6 h pi, most of the cells in the elicited zones contained blue-stained chloroplasts (Fig. 9, *D* and *E*). The staining in chloroplasts became diffuse at 7 h pi, although some color remained in the plasma membrane at this time (Fig. 9*F*). No significant NBT staining was observed in the chloroplasts of leaves inoculated under VLO at any time (not shown).

Similarly, the brown DAB stain marker for H$_2$O$_2$ accumulation was observed in the chloroplasts of both dark- and light-elicited leaves in air, with maximal staining at 4–6 h pi (Fig. 9, *G–I*). In contrast, no significant staining was observed in the chloroplasts of leaves inoculated under VLO (not shown). By 6–7 h pi, a brown precipitate that is characteristic of the peroxidase-mediated reaction with DAB could be observed at the level of plasma membrane of cells elicited in either air (Fig. 9*K*) or VLO (not shown).

Some structural changes were also observed in harpin-elicited mesophyll cells in the presence of DAB. The stain revealed that the chloroplasts were distributed in a regular order around the central vacuole of untreated (not shown) or buffer-infiltrated leaves (Fig. 9*L*). By 5 h post-harpin infiltration, some of the cells were fully plasmolyzed (Fig. 9, *H* and *I*), and by 6–7 h pi, the chloroplasts were virtually undetectable in light-elicited cells (Fig. 9*J*). However, chloroplasts were still visible in some of the dark-elicited cells (Fig. 9*K*).

minated leaves in air, reaching maximal values at 4–5 h pi (Fig. 8). The intensity of the brown coloration was only slightly decreased in dark-elicited leaves. In both cases, the brown stain started to diminish in intensity from 7 to 8 h pi and then gradually disappeared from the inoculated areas. No consistent patterns of DAB staining were observed in buffer-infiltrated leaves. Moreover, very little coloration was observed in harpin-elicited leaves under VLO.

Microscopic examination clearly showed NBT-induced formazan accumulation in cells close to the veins in both buffer- and harpin-treated leaves, at 30 min after harpin treatment in air (Fig. 9, *A* and *B*). A few mesophyll cells (less than 1%) also showed blue staining within the chloroplasts at this time point (Fig. 9*B*, *inset*). The number of mesophyll cells with stained chloroplasts remained very low up to 3 h pi (Fig. 9*C*) and then

These observations indicate that the extent of ROS accumulation in the chloroplasts of harpin-elicited zones was not markedly influenced by light/dark conditions. Small differences in the observations at various points were associated with the slight delay in the execution of the cell death process in the dark. In marked contrast, ROS accumulation was heavily dependent on oxygen availability.

Harpin-induced Changes in Transcript Encoding Antioxidant and Defense Proteins Are Dependent on Environmental Conditions—We have previously described the kinetics of changes in the abundance of mRNAs encoding key cytosolic and organelle-localized antioxidant enzymes during harpin-induced cell death in air in the light (46). We therefore compared the effects of VLO and darkness on the induction of peroxisomal catalase (*CAT*), ascorbate peroxidase (*APX*), and superox-
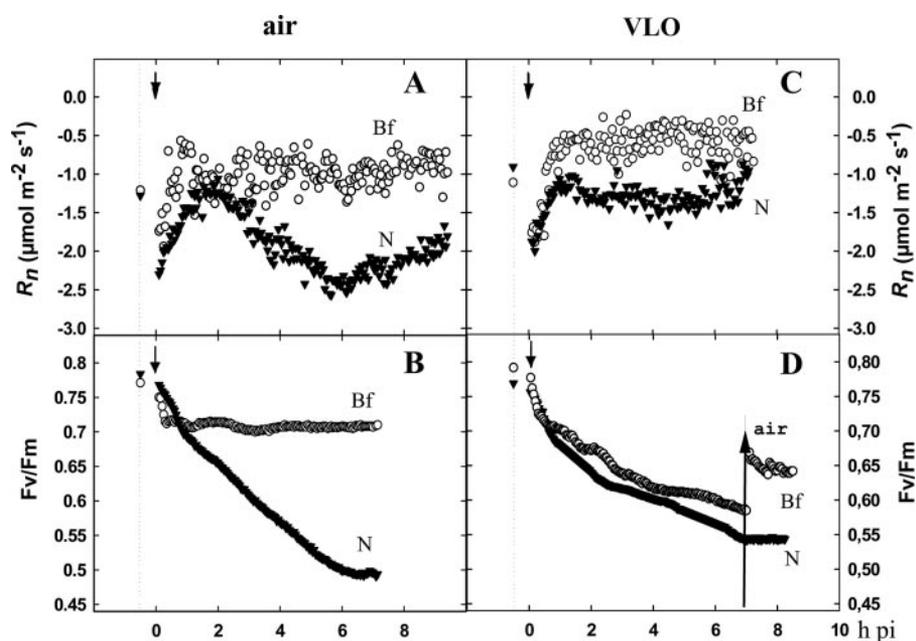
FIGURE 7. **CO_2 release and chlorophyll *a* fluorescence analysis in leaves infiltrated in the dark.** After parameter stabilization (*first symbols* on the *vertical dashed line*) in the dark, in air, or under VLO conditions, leaves were harpin- or buffer-infiltrated, and then infiltrated areas were immediately placed in the gas chambers, as described under "Experimental Procedures." *Arrows*, time infiltration. Data from three independent experiments have been pooled. *Open circles*, buffer (*Bf*); *closed triangles*, harpin (*N*). *A*, CO_2 release in air; *B*, maximum efficiency of PSII photochemistry (F_v/F_m) in air; *C*, CO_2 release under VLO; *D*, F_v/F_m under VLO; the loss of F_v/F_m was partially reversible by returning to air at the 7 h time point (*arrow*) in buffer-treated but not in harpin-treated zones.

ide dismutase (*SOD*) isoforms. At 4 h postelicitation, a marked decline in the abundance of *CAT2*, of the dual targeted chloroplast/mitochondrial *ORGAPX* (47), and of chloroplast *Fe-SOD* transcripts was observed under all conditions (Fig. 10). In contrast, transcript levels of cytosolic *cAPX* and *Cu/Zn-SOD* increased only in the presence of both light and oxygen. It should be noted that the abundance of *cAPX* transcripts was much lower in nonelicited leaves maintained in the dark compared with those exposed to light (data not shown). Thus, accumulation of transcripts encoding cytosolic antioxidants was dependent on both illumination and oxygen, whereas ROS accumulation was only dependent on oxygen. In contrast, transcripts encoding the defense gene phenylalanine ammonialyase (*PAL*), a key enzyme in the synthesis of phenylpropanoid secondary metabolites involved in plant defense (48), accumulated more rapidly under VLO than in air.

DISCUSSION

It is widely accepted that redox processes are central to the initiation and/or execution of plant cell death. However, little information is available in the literature on the precise requirement for oxygen or the relative importance of ROS generated in different plant organelles during the cell death response, particularly ROS generated by photosynthetic and respiratory metabolism. The results presented here demonstrate unambiguously that neither light nor oxygen is essential for harpin-induced cell death. Symptoms were first observed at around 5–6 h pi, and the death process was complete by 48 h pi (Fig. 1). The progression and sequence of the cell death process was the same under all of the conditions (light, dark, air, and VLO)

examined here, as shown by the data on fresh weight measurements and electrolyte leakage (Fig. 2). In addition, the accumulation of transcripts encoding the *Tnt1* transposon, which is considered a good marker of plant stress responses (41), and nuclear fragmentation, a typical PCD response in animals (42), were qualitatively the same in all conditions (Figs. 3–5). Taken together, these observations suggest that the same type of cell death process occurs under all conditions. However, the time course of the death events was affected by light and oxygen availability. These environmental parameters modulate the harpin-induced death reaction in an inverse manner. Darkness delayed the onset of the response, whereas oxygen deprivation accelerated the process (Fig. 2). The relative contributions of chloroplasts and mitochondria to the death process can be assessed by the observed changes in photosynthesis and respiration, together with the localization of ROS accumulation and expression of antioxidant and defense genes.

*Harpin Elicitation Inactivates PSII and Induces ROS Accumulation in the Chloroplasts in both the Light and the Dark—*One of the earliest physiological manifestations of the outcome of the harpin-induced cell suicide program is the loss of photosynthetic capacity (Fig. 6). Early specific effects of the elicitor were observed from 1 h pi. From this time point, the increase in photosynthetic capacity following the initial drop caused by the presence of liquid into the intracellular spaces was delayed in harpin-treated areas compared with zones infiltrated with buffer alone. From 2 h pi, harpin infiltration caused a rapid inhibition of photosynthetic CO_2 assimilation, together with a parallel loss in the yield of PSII reaction centers. Stomatal conductance was not affected before 4 h pi, in good agreement with the previous report on stomatal increase at this time point (49). Thus, the observed inhibition of net photosynthesis was not caused by stomatal limitations on CO_2 availability but rather by down-regulation of the Benson-Calvin cycle and PSII reaction centers. Data in support of this conclusion are provided first by the rapid decrease in F_v/F_m ratio of leaves elicited in the dark (Fig. 7), which is a measure of number of functional PSII centers, and second the observed increases in $(1 - qP)$ values (37). This parameter is a measure of the reduction state of the plastoquinone pool. An increase in $(1 - qP)$ value reflects an impairment of the Benson-Calvin cycle with the resultant decline in use of NADPH and ATP.

Several mechanisms might contribute to the rapid impairment of the Benson-Calvin cycle and PSII activity following harpin elicitation. First, the NBT and DAB data indicate that harpin induces H_2O_2 and superoxide accumulation in the chlo-
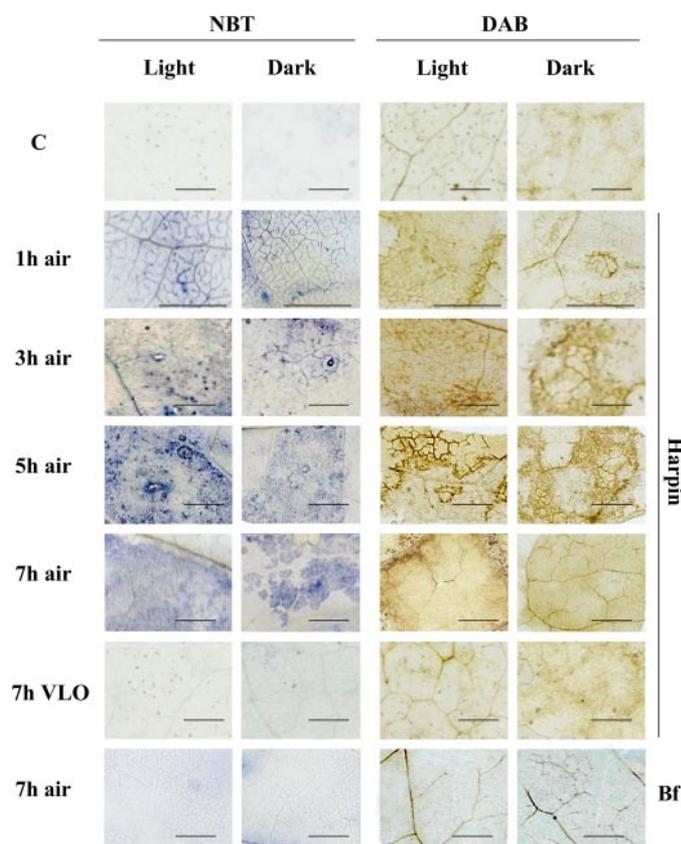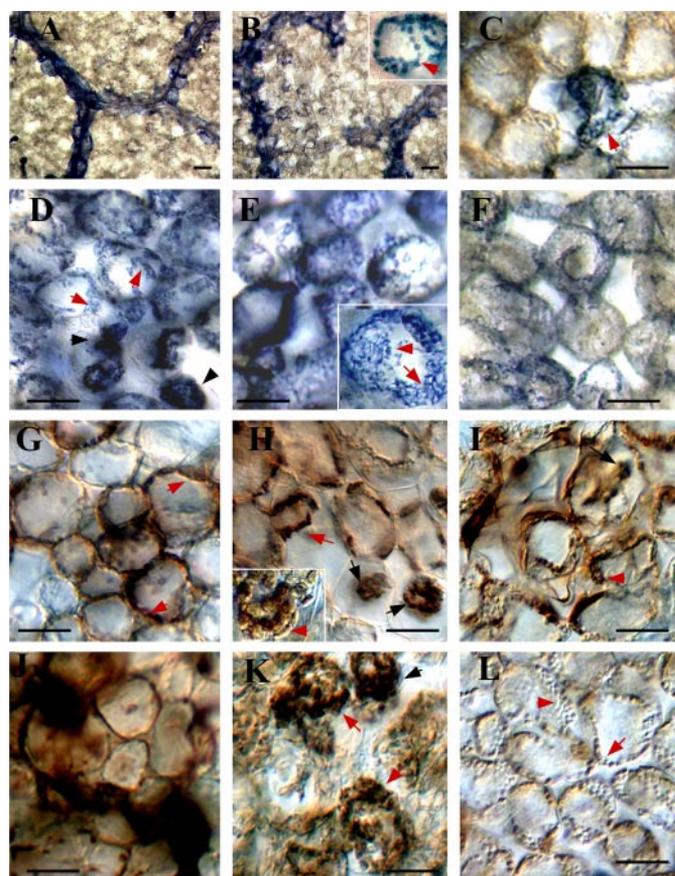
FIGURE 8. *In situ* **detection of ROS after harpin elicitation in different environmental conditions.** Leaves were infiltrated with harpin in the dark or in the light, in air or under VLO conditions. For each sample, treated areas were cut with a scalpel and immediately infiltrated with NBT or DAB staining solutions as described under "Experimental Procedures." The samples shown are representative of at least six independent experiments. *Bf*, buffer; *C*, untreated leaves in air. *Bars*, 6 mm.

FIGURE 9. **Microscopic detection of ROS after harpin elicitation in the light and the dark under atmospheric oxygen.** Leaves were infiltrated with harpin or buffer in the dark or in the light, and treated areas were immediately placed in staining solutions as described under "Experimental Procedures" (*cf.* Fig. 8). *Colored areas* were then observed under an optical Zeiss microscope. *A–F*, NBT staining; *G–L*, DAB staining. *A*, buffer 30 min pi; *B*, harpin 30 min pi. *Inset*, isolated cell with blue-colored chloroplasts; *C*, harpin 3 h pi, light; *D*, harpin 5 h pi, light; *E*, harpin 5 h pi, dark; *inset*, enlargement (×2); *F*, harpin 7 h pi, light; *G*, harpin 3 h pi, light; *H*, harpin 5 h pi, light; *inset*, enlargement (×2); *I*, harpin 5 h pi, dark; *J*, harpin 7 h pi, light; *K*, harpin 7 h pi, dark; *L*, buffer 5 h pi, light. *Red arrows*, chloroplasts; *black arrows*, collapsed cells. *Bars*, 100 μm.

roplasts (Fig. 9). Although the results of such staining procedures must be interpreted with caution (44), the maximum intensity of staining occurred at around 4–6 h post-harpin inoculation, strongly suggesting ROS accumulation. As little as 10 μM H_2O_2 will inhibit CO_2 assimilation by over 50%, through inactivation of the thiol-modulated Benson-Calvin cycle enzymes (51). H_2O_2 can also interact directly with the oxygen-evolving complex of PSII and other electron transport components and impair the function of the PSII turnover and repair cycle involving the removal of light-damaged D1 proteins and reinsertion of new function D1 proteins (52).

The second mechanism that could result in a rapid inhibition of photosynthesis following harpin elicitation involves specific changes to the organization of the thylakoid membranes. This is suggested by the harpin-induced modifications in the reflective index of the membranes observed by optical coherence tomography (53). Stress-induced changes in the organization of thylakoid structure and composition can decrease PSII and photosystem I activities (54). Since kinase activities are induced early (less than 30 min) after harpin elicitation (55), they may contribute to the inactivation of PSII function that commences 2 h pi.

A third explanation for the rapid impairment of photosynthesis could be alterations in the abundance, composition, or regulated function of components downstream of PSII in the photosynthetic electron transport chain. Since harpin induces

ferredoxin kinase activity in *in vitro* assays (56), it is entirely possible that ferredoxin reductase and other enzymes associated with ferredoxin-mediated are modulated during the death response. The observation that transgenic tobacco with reduced ferredoxin levels are more susceptible to pathogens (57) is consistent with this hypothesis.

The three mechanisms described above are not mutually exclusive and may act synergistically. Indeed, the inhibition of the PSII repair cycle by ROS is accelerated by inhibition of the Benson-Calvin cycle (58). However, the precise origins of the ROS accumulation observed in the mesophyll chloroplasts (Fig. 9) remain to be determined. Indeed, whereas the chloroplast ETC uses oxygen as an electron acceptor producing superoxide and hence H_2O_2, this process is light-dependent, and hence it cannot explain the accumulation of ROS in the dark (Fig. 9). ROS accumulation in the dark could be linked to specific enhancement of NADPH oxidase-like enzymes, as reported for harpin-elicited suspension cells (27, 59). However, these enzymes are generally considered to function in the plasmalemma, and it is highly unlikely that H_2O_2 can pass freely from the apoplast to the cytosol
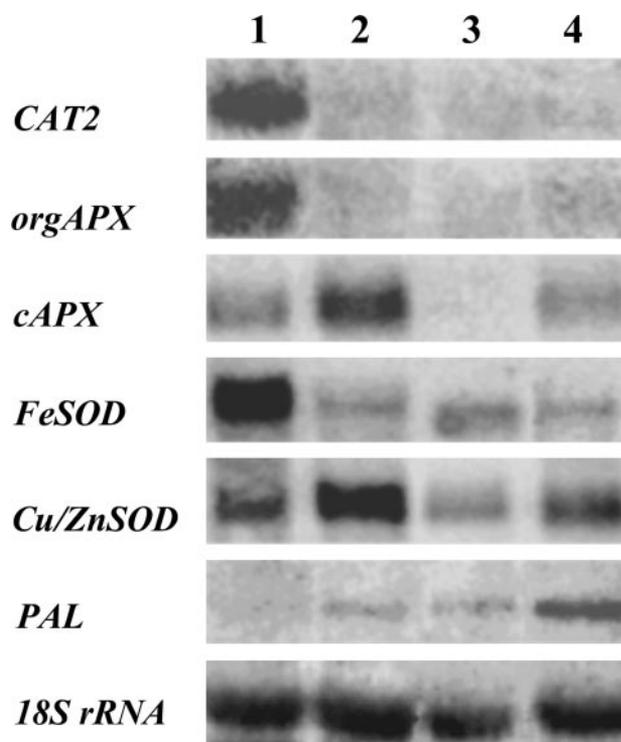
FIGURE 10. **Expression of antioxidant and defense genes after harpin elicitation in different environmental conditions.** Northern blot analyses of transcripts encoding peroxisomal CAT2, organellar APX (*orgAPX*), chloroplastic Fe-SOD, cytosolic cAPX, cytosolic CuZn-SOD, phenylalanine ammonia-lyase PAL, 4 h post-harpin infiltration. *Lane 1*, untreated leaf in the light under air; *lane 2*, harpin-infiltrated leaf in the light under air; *lane 3*, harpin-infiltrated leaf in the dark under air; *lane 4*, harpin-infiltrated leaf in the light under VLO. The 18 S rRNA was detected as a standard for relative loading. Results shown are representative of at least three independent experiments.

and then to the chloroplasts, given the high reactivity of this compound with protein thiol groups and cytosolic antioxidants. However, H_2O_2 can be transported into the cytosol by the aquaporins (60). It is also possible that the accumulation of superoxide in chloroplasts is due to the activation of the thylakoid NADPH oxidase complex in response to PCD triggers or to the NADPH oxidase-like activities previously reported to be associated with the chloroplast envelope (61). Proteomic studies have also revealed that novel proteins become associated with the chloroplast envelope following exposure to stress (62).

The rapid decline in *orgAPX* and *Fe-SOD* transcripts occurring 4 h after harpin elicitation in both the light and the dark (Fig. 10) could contribute to the accumulation of ROS in the chloroplasts. Transcripts encoding the major leaf peroxisomal catalase isoforms, *CAT2* (Fig. 10) and *CAT1* (46), were also greatly decreased. Moreover, there was a 2-fold decrease in the ascorbate depletion-sensitive chloroplastic APX and in CAT activities at 6 h pi (85),[5] indicating a loss of capacity for hydrogen peroxide scavenging in both chloroplasts and peroxisomes.

Recent models have proposed that ROS produced by the chloroplast ETC are key to the signaling of responses to both biotic and abiotic stresses (14, 15, 63). However, this is clearly not the case in the harpin-induced cell death process, where darkness had only limited effects on both ROS accumulation in

the chloroplasts and the establishment of cell death. Hence, light-mediated processes are not as important in harpin-induced cell death as they are in other systems that trigger plant cell death, which are more or less completely light-dependent.

Oxygen Deprivation Interferes with the PCD Process by Limiting Production of Extramitochondrial ROS and Favoring ROS Accumulation in the Mitochondrial Matrix—The negative interactions of ROS with the photosynthetic processes can explain the delayed decline in both PSII and maximum yield of PSII photochemistry (F_v/F_m) after harpin inoculation under VLO (Fig. 6, *E* and *G*). In addition, VLO almost abolishes the CO_2 burst occurring in dark-elicited leaves in air, which reached a maximum at 4–8 h pi (Fig. 7*C*). Although a small amount of CO_2 might be produced by fermentation under aerobic conditions, the inhibition of the CO_2 burst under VLO shows that the majority of the CO_2 arises from the tricarboxylic acid cycle. Moreover, harpin induces a 2-fold increase in oxygen uptake rates in light-elicited leaves (23). The bursts in CO_2 release in dark-elicited leaves (Fig. 7*A*) and in oxygen uptake in light-elicited leaves (23) are co-incident, both peaking at 6–8 h pi. The harpin-induced oxygen burst in the light has been reported to be sustained by a 5-fold increase in AOX activity, with only a 50% increase in the activity of the cytochrome (COX) pathway (23). The increased AOX activity might be predicted to protect mitochondrial function by minimizing superoxide generation at the level of Complexes I and III (64). This view is consistent with the known sensitivities of the tricarboxylic acid cycle and respiratory enzymes to hydrogen peroxide (65, 66). Although our results suggest that AOX is induced to a similar extent in the dark and the light, the actual rate of flux through the alternative pathway can only be measured by oxygen isotope discrimination (67), and such measurements are therefore beyond the scope of the present study. However, our current knowledge of the relative affinities of AOX and cytochrome oxidase for oxygen would predict that oxygen deprivation should limit AOX activity much more than COX activity. Indeed, the K_m of AOX for oxygen, which is around 20 μM (equivalent to around 1% of the air levels of O_2) (68, 69) is much higher than that of Complex III, which is around 0.14 μM (equivalent to only 0.01% of the air levels of O_2). The observed impairment of the CO_2 burst under VLO in the dark (Fig. 7*C*) is thus likely to be caused by the inhibition of AOX activity.

Moreover, it is logical to presume that ROS generation via respiratory electron flow (mitochondrial ROS) is actually increased under VLO, since the probability of electron donation to oxygen is enhanced when respiratory electron acceptors become overreduced. The potential for superoxide production increases in these circumstances, as has been shown in several animal hypoxic systems (70, 71). Hence, mitochondrial ROS are likely to accumulate in harpin-elicited leaves under VLO and might contribute to the higher cell death rates. These results are in good agreement with the hypothesis that the mitochondrial ETC acts as an oxygen sensor such that mitochondria are able to detect oxygen deprivation (72, 73). In contrast, the accumulation of ROS in the chloroplasts seems to be less important, since both DAB and NBT staining are prevented under VLO (Fig. 9). The lack of DAB staining could be due in part to the inhibition of peroxidase activity, but this is not the case for NBT

---

[5] M. Garmier, unpublished results.

staining that does not depend on the presence of oxygen. Our data also challenge the roles for apoplastic ROS produced by plasmamembrane NADPH oxidases and peroxidases in the execution of cell death. These enzymes are involved in ROS generation during mild hypoxic stress (72, 74). However, the conditions of severe oxygen deprivation applied here (<0.1% O_2) should markedly repress NADPH oxidase activity, which has a K_m of around 5–10 μM (corresponding to 0.2–0.5% O_2) (75). A study with inhibitors has already suggested that NADPH oxidase activities are not necessary for harpin-induced cell death in tobacco suspension cultures (76). In good agreement with this hypothesis, ROS accumulation was decreased under VLO (Figs. 8 and 9), as was the abundance of transcripts encoding cytosolic antioxidants, such as Cu/Zn-SOD and cAPX (Fig. 10). Accumulation of these transcripts is generally considered to be a good marker of ROS availability in the cytoplasm (77, 78). In contrast, *PAL* (Fig. 10) and *Tnt1* (Fig. 3) transcripts were more enhanced at 4 h pi under VLO than in air. The independent induction of ROS, antioxidants, and defense systems alongside the localized PCD responses is characteristic for a number of plant/pathogen interactions (79, 80).

The inverse effects on intracellular localization of ROS accumulation could have important consequences for redox gradients across membranes and the partitioning of redox signals. This localized partitioning of ROS generation/accumulation and associated effects on cellular redox homeostasis may be as important in plant/pathogen interactions as they are in the stress responses to excess light, where ROS are, however, prominent players (14, 15). During elicitor-induced cell death, extramitochondrial ROS may actually counteract the PCD process, by inducing basal resistance. Indeed, like flagellins, harpin proteins are considered as microbe-associated molecular patterns that elicit basal defense responses (81). However, harpin N_{Ea} is involved in the hypersensitive response-eliciting capacity of *E. amylovora* in nonhost plants and produces cellular events that are biologically relevant and that are common to plant programmed cell death signatures (24, 26). Microbial associated molecular patterns and pathogen effectors probably use similar signaling cascades, since they both trigger the redox-modulated NPR1-mediated pathways of defense gene expression. In this way, both effectors and microbial associated molecular patterns contribute to SAR initiation (82). It would thus be of interest to know whether the redox signaling cascades, particularly the NPR1 pathway, are accelerated during the death process under VLO. Moreover, it would be interesting to determine whether the same cellular responses that we report here also occur following elicitation by *E. amylovora*, particularly the acceleration of the death process under low oxygen. However, this could be difficult to assess experimentally, because oxygen deprivation is likely to affect bacterial growth.

Different pathways of cell death signaling that involve both ROS-dependent and ROS-independent processes are likely to co-exist in plants (83) as in other organisms (84). Chloroplasts and mitochondria probably have other roles in plant/pathogen interactions in addition to ROS generation, particularly since both organelles are essential contributors to cell metabolism. Roles for metabolic interplay and sugar sensing in particular have been described in both virulent and avirulent plant/patho-gen interactions (13). It has been suggested that photosynthesis and assimilatory metabolism are switched off in order to initiate respiration and defense reactions (12). However, if this were the case in the harpin-induced cell death, one would predict that the process should be more rapid in the dark than in the light, whereas the inverse situation was observed. Moreover, the regulated decreases in photosynthesis (Fig. 6) were markedly delayed by VLO, whereas cell death was accelerated (Fig. 2). However, the availability of ATP is of major importance, since it supports the activities of many key enzymes, at least by comparison with the ATP-dependent enzymes that are involved in the execution of the cell death process in animals (84). Chloroplast-generated ATP is essentially consumed within the organelle during the turnover of the Benson-Calvin cycle, which generates triose-phosphates for carbohydrate formation, including starch synthesis. In contrast, mitochondrial ATP is largely exported to the cytosol, where it contributes to general cell metabolism (50). A role for ATP generation in plant PCD has been suggested by studies involving modeling of mitochondrial ATP formation during harpin-induced cell death in the light (23). The 2-fold increase in respiration induced by harpin in darkness under VLO compared with buffer-treated leaves (Fig. 7C) would mainly reflect cytochrome oxidase activity, as discussed above, and would be sufficient to sustain efficient ATP production. Moreover, the photosynthetic production of carbon skeletons by the chloroplast in the light, which continues during the initial period after elicitation, would help to sustain mitochondrial respiration. The need for photosynthetic production of the substrates required for oxidation in respiration might explain, at least in part, why the higher rates of cell death are observed under both VLO and illumination (Fig. 2).

In conclusion, we have shown that although extramitochondrial ROS are not crucial to the execution of harpin N_{Ea}-induced cell death, mitochondrial redox signals, including mitochondrial ROS, and metabolic interactions between chloroplasts and mitochondria could play a major role in the execution of the regulated cell suicide program.

REFERENCES

1. Pitzschke, A., and Hirt, H. (2006) *Plant Physiol.* **141,** 351–356
2. Hail, N., Jr., Carter, B.Z., Konopleva, M., and Andreef, M. (2006) *Apoptosis* **11,** 889–904
3. Basset, G., Raymond P., Malek L., and Brouquisse, R. (2002) *Plant Physiol.* **128,** 1149–1162
4. Lamb, C., and Dixon, D. A. (1997) *Annu. Rev. Plant Physiol. Plant Mol. Biol.* **48,** 251–275
5. Sagi, M., and Fluhr, R. (2001) *Plant Physiol.* **126,** 1281–1290
6. Bolwell, G. P., Bindschedler, L. V., Blee, K. A., Butt, V. S., Davies, D. R., Gardner, S. L., Gerrish, C., and Minibayeva, F. (2002) *J. Exp. Bot.* **53,** 1367–1376
7. Torres, M. A., Jones, J. D., and Dangl, J. L. (2005) *Nat. Genet.* **37,** 1130–1134
8. Foyer, C. H., and Noctor, G. (2000) *New Phytol.* **146,** 359–388
9. Foyer, C. H., and Noctor, G. (2005) *Plant Cell Environ.* **29,** 1056–1071
10. Lawlor, D. W., and Cornic, G. (2002) *Ann. Bot.* **89,** 887–894

11. Matsumura, H., Reich, S., Ito, A., Saitoh, H., Kamoun, S., Winter, P., Kahl, G., Reuter, M., Kruger, D. H., and Terauchi, R. (2003) *Proc. Natl. Acad. Sci. U. S. A.* **100,** 15718 –15723
12. Scharte, J., Schön, H., and Weis, E. (2005) *Plant Cell Environ.* **28,** 1421–1435
13. Bonfig, K. B., Schreiber, U., Gabler, A., Roitsch, T., and Berger, S. (2006) *Planta* **225,** 1–12
14. Karpinski, S., Gabrys, H., Mateo, A., Karpinska, B., and Mullineaux, M. (2003) *Curr. Opin. Plant Biol.* **6,** 390–396
15. Bechtold, U., Karpinski, S., and Mullineaux, P. M. (2005) *Plant Cell Environ.* **28,** 1046–1055
16. Sweetlove, L., and Foyer, C. H. (2004) in *Plant Mitochondria: From Genome to Function* Vol. 17 (Day, D. A., Millar, A. H., and Whelan, J., eds) pp. 307–320
17. Lam, E., Kato, N., and Lawton, M. (2001) *Nature* **411,** 848 – 853
18. Desagher, S., and Martinou, J. C. (2000) *Trends Cell Biol.* **10,** 369 –377
19. Curtis, M. J., and Wolpert, T. J. (2002) *Plant J.* **29,** 295–312
20. Purvis, A. C. (1997) *Physiol. Plant.* **100,** 165–170
21. Simons, B. H., Millenaar, F. F., Mulder, L., Van Loon, L. C., and Lambers, H. (1999) *Plant Physiol.* **120,** 529 –538
22. Clifton, R., Millar, A. H., and Whelan, J. (2006) *Biochim. Biophys. Acta* **1757,** 730 –741
23. Vidal, G., Ribas-Carbo, M., Garmier, M., Dubertret, G., Rasmusson, A. G., Mathieu, C., Foyer, C. H., and De Paepe, R. (2007) *Plant Cell* **19,** 640 – 655
24. Wei, Z. M., Laby, R. J., Zumoff, C. H., Bauer, D. W., He, S. Y., Collmer, A., and Beer, S. V. (1992) *Science* **257,** 85– 88
25. He, S. Y., Yang, H. C., and Collmer, A. (1993) *Cell* **73,** 1255–1266
26. Oh, C. S., and Beer, S. V. (2005) *FEMS Microbiol. Lett.* **253,** 185–192
27. Baker, C. J., Orlandi, E. W., and Mock, N. M. (1993) *Plant Physiol.* **102,** 1341–1344
28. Samuel, M. A., Hall, H., Krzymowska, M., Drzewiecka, K., Hennig, J., and Ellis, B. E. (2005) *Plant J.* **42,** 406 – 416
29. Dong, H., Delaney, T. P., Bauer, D. W., and Beer, S. V. (1999) *Plant J.* **20,** 207–215
30. He, S. Y., Bauer, D. W., Collmer, A., and Beer, S. V. (1994) *Mol. Plant Microbe Interact.* **7,** 289 –292
31. Xie, Z., and Chen, Z. (2000) *Mol. Plant Microbe Interact.* **13,** 183–190
32. Krause, M., and Durner, J. (2004) *Mol. Plant-Microbe Interact.* **17,** 131–139
33. Gaudriault, S., Brisset, M. N., and Barny, M. A. (1998) *FEBS Lett.* **428,** 224 –228
34. Pike, S. M., Adam, A. L., Pu, X. A., Hoyos, M. E., Laby, R., Beer, S. V., and Novacky, A. (1998) *Physiol. Mol. Plant Pathol.* **53,** 39 – 60
35. Dutilleul, C., Driscoll, S., Cornic, G., De Paepe, R., Foyer, C. H., and Noctor, G. (2003) *Plant Physiol.* **131,** 264 –275
36. Schreiber, U., Schliwa, U., and Bilger, W. (1986) *Photosynth. Res.* **10,** 51– 62
37. Genty, B., Briantais, J. M., and Baker, N. R. (1989) *Biochim. Biophys. Acta* **990,** 87–92
38. Dutilleul, C., Garmier, M., Noctor, G., Mathieu, C., Chétrit, P., Foyer, C. H., and De Paepe, R. (2003) *Plant Cell* **15,** 1212–1226
39. Dietrich, P., Sanders, D., and Hedrich, R. (2001) *J. Exp. Bot.* **52,** 1959 –1967
40. Drew, M. C. (1997) *Annu. Rev. Plant Physiol. Plant Mol. Biol.* **48,** 223–250
41. Pouteau, S., Grandbastien, M. A., and Boccara, M. (1994) *Plant J.* **5,** 535–542
42. Lu, C., Zhang, C., and Zhai, Z. (2005) *Proc. Natl. Acad. Sci. U. S. A.* **102,** 2778 –2783
43. Li, Y.-M., Mackintosh, C., and Casida, J. E. (1993) *Biochem. Pharmacol.* **46,** 1435–1443
44. Shulaev, V., and Oliver, D. J. (2006) *Plant Physiol.* **141,** 367–372
45. Dat, J. F., Pellinen, R., Beeckman, T., Van De Cotte, B., Langebartels, C., Kangasjarvi, J., Inzé, D., and Van Breusegem, F. (2003) *Plant J.* **33,** 621– 632
46. Garmier, M., Dutilleul, C., Mathieu, C., Chétrit, P., Boccara, M., and De Paepe, R. (2002) *Plant Physiol. Biochem.* **40,** 561–566
47. Chew, O., Whelan, J. W., and Millar, A. H. (2003) *J. Biol. Chem.* **278,** 46869 –46877
48. Draper, J. (1997) *Trends Plant Sci.* **2,** 162–165
49. Boccara, M., Boué, C., Garmier, M., De Paepe, R., and Boccara, A. C. (2001) *Plant J.* **28,** 663 – 670
50. Igamberdiev, A. U., Hurry, V., Krömer, S., and Gardeström, P. (1998) *Physiol. Plant.* **104,** 431– 439
51. Kaiser, W. (1979) *Planta* **145,** 377– 382
52. Zhang, L., and Aro, M. A. (2002) *FEBS Lett.* **512,** 13–18
53. Boccara, M., Schwartz, W., Guiot, E., Vidal, G., De Paepe, R., Dubois, A., and Boccara, A. C. (2007) *Plant J.* **50,** 338 –346
54. Allen, J. F., and Forsberg, J. (2001) *Trends Plant Sci.* **6,** 317–326
55. Adam, A. L., Pike, S., Hoyos, M. E., Stone, J. M., Walker, J. C., and Novacky, A. (1997) *Plant Physiol.* **115,** 853 – 861
56. Huang, H.-E., Ger, M.-J., Chen, C.-Y., Pandey, A.-K., Yip, M. K., Chou, H.-W., and Feng, T.-Y. (2007) *Mol. Plant Pathol.* **8,** 129 –137
57. Dayakar, B. V., Lin, H., Chen, C., Ger, M., Lee, B. H., Pai, C., Chow, D., Huang, H., Hwang, S., Chung, M., and Feng, T. (2003) *Plant Mol. Biol.* **51,** 913 –924
58. Takahashi, T., and Murata, N. (2005) *Biochim. Biophys. Acta* **1703,** 352–361
59. Andi, S., Taguchi, F., Toyoda, K., Shiraishi, T., and Ichinose, Y. (2001) *Plant Cell Physiol.* **42,** 446 – 449
60. Bienert, G. P., Møller, A. L. B., Kristiansen, K. A., Schulz, A., Møller, I. M., Schjoerring, J. K., and Jahn, T. P. (2007) *J. Biol. Chem.* **282,** 1183–1192
61. Jäger-Vottero, P., Dorne, A. J., Jordanov, J., Douce, R., and Joyard, J. (1997) *Proc. Natl. Acad. Sci. U. S. A.* **94,** 1597–1602
62. Ferro, M., Salvi, D., Brugiere, S., Miras, S., Kowalski, S., Louwagie, M., Garin, J., Joyard, J., and Rolland, N. (2003) *Mol. Cell. Proteomics* **2,** 325–345
63. Liu, Y., Reng, D., Pike, S., Pallardy, S., Gassmann, W., and Zhang, S. (2007) *Plant J.* **51,** 941–954
64. Møller, I. M. (2001) *Annu. Rev. Plant Physiol. Plant Mol. Biol.* **52,** 561–591
65. Verniquet, F., Gaillard, J., Neuberger, M., and Douce, R. (1991) *Biochem. J.* **276,** 643– 648
66. Nulton-Persson, A. C., and Szweda, L. I. (2001) *J. Biol. Chem.* **276,** 23357–23361
67. Ribas-Carbo, M., Berry, J. A., Yakir, D., Giles, L., Robinson, S. A., Lennon, A. M., and Siedow, J. N. (1995) *Plant Physiol.* **109,** 829 – 837
68. Millar, A. H., Bergensen, F. J., and Day, D. A. (1994) *Plant Physiol. Biochem.* **32,** 847– 852
69. Ribas-Carbo, M., Berry, J. A., Azcon-Bieto, J., and Siedow, J. N. (1994) *Biochim. Biophys. Acta* **1188,** 205–212
70. Chandel, N. S., McClintock, D. S., Feliciano, C. E., Wood, T. M., Melendez, J. A., Rodriguez, A. M., and Schumacker, P. T. (2000) *J. Biol. Chem.* **275,** 25130 –25138
71. Brunelle, J. K., Bell, E. L., Quesada, N. M., Verkauteren, K., Tiranti, V., Zeviani, M., Scarpulla, R. C., and Chandel, N. S. (2005) *Cell Metab.* **1,** 409 – 414
72. Bailey-Serres, J., and Chang, R. (2005) *Ann. Bot.* **96,** 507–518
73. Kemp, P. J. (2006) *Exp. Physiol.* **91,** 829 – 834
74. Blokhina, O. B., Chirkova, T. V., and Fagerstedt, K. V. (2001) *J. Exp. Bot.* **52,** 1179 –1190
75. Cross, A. R., and Segal, A. W. (2004) *Biochim. Biophys. Acta* **1657,** 1–22
76. Ichinose, Y., Andi, S., Doi, R., Tanaka, R., Taguchi, F., Sasabe, M., Toyoda, K., Shiraishi, T., and Yamada, T. (2001) *Plant Physiol. Biochem.* **39,** 771–776
77. Karpinski, S., Escobar, C., Karpinska, B., Creissen, G., and Mullineaux, P. M. (1997) *Plant Cell* **9,** 627– 640
78. Foyer, C. H., and Noctor, G. (2003) *Physiol. Plant.* **119,** 355–364
79. Jakobek, J. L., and Lindgren, P. B. (1993) *Plant Cell* **5,** 49 –56
80. Torres, M. A., Jones, D. G., and Dangl, J. L. (2006) *Plant Physiol.* **141,** 373–378
81. Bent, A., and Mackey, D. (2007) *Annu. Rev. Phytopathol.* **45,** 17.1–17.38
82. Mishina, T. E., and Zeier, J. (2007) *Plant J.* **50,** 500 –513
83. Baek, D., Nam, J., Koo, Y. D., Kim, D. H., Lee, J., Jeong, J. C., Kwak, S. S., Chung, W. S., Lim, C. O., Bahk, J. D., Hong, J. C., Lee, S. Y., Kawai-Yamada, M., Uchimiya, H., and Yun, D. J. (2004) *Plant Mol. Biol.* **56,** 15–27
84. Ameisen, J. C. (2002) *Cell Death Differ.* **9,** 367–393
85. Garmier, M. (2003) *Implication of Plant Mitochondria in Cellular Redox State and Responses to Biotic Stress*, Ph. D. thesis, Université Paris-Sud XI, Orsay, France

Light and Oxygen Are Not Required for Harpin-induced Cell Death

Marie Garmier, Pierrick Priault, Guillaume Vidal, Simon Driscoll, Reda Djebbar, Martine Boccara, Chantal Mathieu, Christine H. Foyer and Rosine De Paepe

Access the most updated version of this article at doi: 10.1074/jbc.M707226200

Alerts:
- When this article is cited
- When a correction for this article is posted

Click here to choose from all of JBC's e-mail alerts

This article cites 84 references, 24 of which can be accessed free at
http://www.jbc.org/content/282/52/37556.full.html#ref-list-1